

Discovery of Key Dioxygenases that Diverged the Paraherquonin and Acetoxydehydroaustin Pathways in *Penicillium brasilianum*

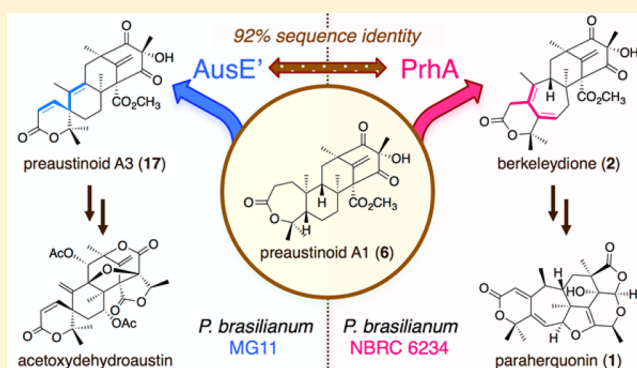
Yudai Matsuda,^{†,‡} Taiki Iwabuchi,^{†,‡} Takayuki Fujimoto,[†] Takayoshi Awakawa,[†] Yu Nakashima,[†] Takahiro Mori,[†] Huiping Zhang,[§] Fumiaki Hayashi,[§] and Ikuro Abe^{*,†}

[†]Graduate School of Pharmaceutical Sciences, The University of Tokyo, 7-3-1 Hongo, Bunkyo-ku, Tokyo 113-0033, Japan

[§]RIKEN Center for Life Science Technologies, 1-7-22 Suehiro-cho, Tsurumi-ku, Yokohama, Kanagawa 230-0045, Japan

Supporting Information

ABSTRACT: Paraherquonin (**1**), a fungal meroterpenoid produced by *Penicillium brasilianum* NBRC 6234, possesses a unique, highly congested hexacyclic molecular architecture. Here we identified the biosynthetic gene cluster of **1** (the *prh* cluster) and elucidated the pathway up to berkeleydione (**2**), which serves as the key intermediate for the biosynthesis of **1** as well as many other meroterpenoids. Interestingly, the nonheme iron and α -ketoglutarate-dependent dioxygenase PrhA constructs the cycloheptadiene moiety to afford **2** from preaustinoide A1 (**6**), probably via the homoallyl-homoallyl radical rearrangement. Additionally, another fungal strain, *P. brasilianum* MG11, which produces acetoxydehydroaustin instead of **1**, was found to have a gene cluster nearly identical to the *prh* cluster. The dioxygenase encoded by the cluster shares 92% sequence identity with PrhA, and also accepts **6** but produces preaustinoide A3 (**17**) with a spiro-lactone system, generating a diverging point for the two different meroterpenoid pathways in the same species.



INTRODUCTION

3,5-Dimethylorsellinic acid (DMOA), an aromatic polyketide widely produced by fungi, especially in the family Aspergillaceae, is further transformed into many intriguing meroterpenoids, in terms of both chemical structures and biological activities.^{1,2} Recent studies revealed the molecular basis for the biosyntheses of some DMOA-derived meroterpenoids,^{3–10} and demonstrated that oxidative enzymes are the key components for their structural complexification. However, many reactions and enzymes still remain to be discovered.²

Paraherquonin (**1**) is a DMOA-derived meroterpenoid isolated from *Penicillium brasilianum* (synonym: *P. paraherquei*) NBRC 6234, and possesses a unique and congested hexacyclic skeleton.¹¹ Analogues of **1** have been isolated from several fungi in the genus *Penicillium*, including berkeleyacetals,¹² miniolutelides,¹³ and dhilirolides^{14,15} (Figure 1A). Although none of the biosyntheses of the above-described molecules have been investigated at the genetic level, all of them appear to be derived from the common intermediate, berkeleydione (**2**).^{16,17} Interestingly, **2** and berkeleyacetals reportedly inhibit matrix metalloproteinase-3 and caspase-1,^{12,16} and among them, berkeleyacetal C exhibits anti-inflammatory activity as well.¹⁸ In contrast, dhilirolides exhibit insecticidal activity.¹⁵ Thus, the biosynthetic studies of berkeleydione should definitely contribute toward clarifying the bioprocesses underlying the syntheses of many important natural products.

In this study, we discovered the biosynthetic gene cluster for paraherquonin (**1**) in *P. brasilianum* NBRC 6234 (the *prh* cluster), and characterized the four oxidative enzymes responsible for the generation of berkeleydione (**2**). Notably, the nonheme iron-dependent dioxygenase PrhA catalyzes the cycloheptadiene formation to yield **2**. Intriguingly, another strain (*P. brasilianum* MG11) has a homologous gene cluster to the *prh* cluster encoding a predicted dioxygenase that is almost identical to PrhA (the *aus'* cluster), but reportedly produces acetoxydehydroaustin and other related compounds instead of **1** (Figure 1B). Our analyses revealed that the homologous dioxygenase encoded by the *aus'* cluster shares its substrate with PrhA but produces a different product with a spiro-lactone moiety, diverging the metabolic pathways for the two different compounds in the same species.

RESULTS AND DISCUSSION

Discovery and Bioinformatic Analysis of the Paraherquonin Biosynthetic Gene Cluster. To obtain the biosynthetic gene cluster for paraherquonin (**1**), we initially performed the whole genome sequencing of *P. brasilianum* NBRC 6234, a known producer of **1**.¹¹ As previously proposed, the early stage in the biosynthesis of **1** should resemble that of austinol,² which is synthesized by the *aus* cluster in *Aspergillus*

Received: August 11, 2016

Published: September 7, 2016

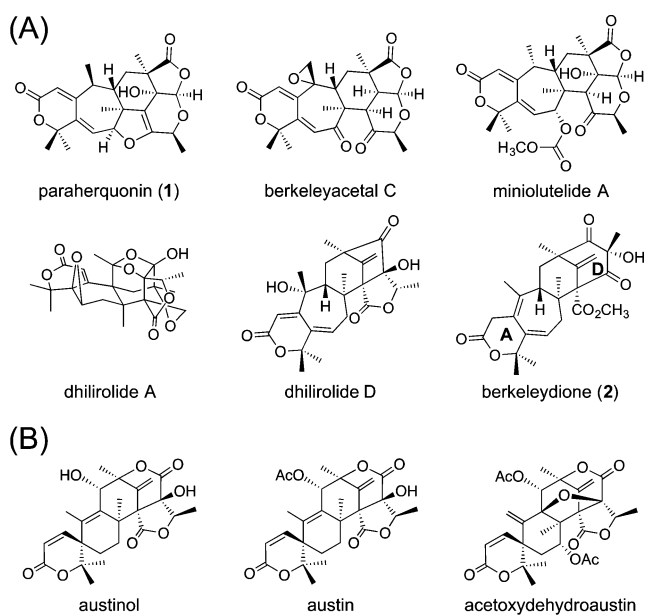


Figure 1. (A) Structures of paraherquonin (1) and related fungal meroterpenoids presumably derived from berkeleydione (2). (B) Selected meroterpenoids isolated from *P. brasilianum* MG11.

nidulans.^{3,8,19} Thus, we searched for a genomic region encoding enzymes homologous to those encoded by the *aus* cluster. We found a putative biosynthetic gene cluster for 1, which consists of 14 genes altogether and was designated as the *prh* cluster (Figures 2 and S4; DDBJ/EMBL/GenBank accession number:

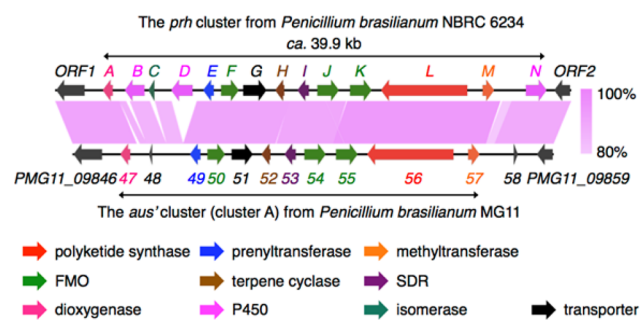


Figure 2. Schematic representation of the *prh* cluster and its nucleotide sequence comparison with the *aus'* cluster from *P. brasilianum* MG11. The illustration of the sequence comparison was illustrated using easyFig.²⁰

LC127182). The boundaries of the cluster were assigned on the basis of the fact that the products of the flanking genes (*ORF1* and *ORF2*) are apparently not essential for the paraherquonin biosynthesis and that their close homologues (with >70% protein sequence identity) can be found in many other fungi (Figure S4). On the basis of the predicted functions of the cluster-encoded proteins, the first five steps of the biosynthesis of 1 should be identical to those of austinol: the PKS PrhL synthesizes DMOA, which is followed by farnesylation by the prenyltransferase PrhE, methylesterification by the methyltransferase PrhM, epoxidation of the prenyl chain by the flavin-dependent monooxygenase (FMO) PrhF, and cyclization of the farnesyl moiety by the terpene cyclase PrhH, to yield the tetracyclic intermediate, protoaustinoide A (3).

The *prh* cluster encodes eight putative tailoring enzymes including one Fe(II)/ α -ketoglutarate (α -KG)-dependent diox-

xygenase (PrhA), three cytochrome P450 monooxygenases (PrhB, PrhD, and PrhN), one isomerase (PrhC), one short-chain dehydrogenase/reductase (SDR; PrhI), and two FMOs (PrhJ and PrhK). Although no protein homologous to the SDR PrhI has been found in the austinol pathway, close homologues of PrhI are utilized in the biosyntheses of several other meroterpenoids, and they all oxidize the C-3 alcohol group of the terpene cyclase product to the corresponding ketone.^{6,7,9,10}

We therefore reasoned that PrhI accepts the cyclized product 3 and performs the C-3 oxidation to provide 4 (Scheme 1). The next two conversions would involve two FMOs, PrhJ and PrhK, which are similar to AusB and AusC, respectively. Since AusB and AusC are engaged in C-5' hydroxylation and Baeyer–Villiger oxidation, respectively,⁸ it is most likely that PrhJ and PrhK have the same functions and generate preaustinoide A²¹ (5) and preaustinoide A1²² (6) from 4. In the austinol pathway, 6 then undergoes two successive oxidations catalyzed by the Fe(II)/ α -KG-dependent dioxigenase AusE to yield preaustinoide A3 (17) with a spiro-lactone system via preaustinoide A2 (16).⁸ The *prh* cluster indeed encodes a protein homologous to AusE, PrhA, which shares 78% sequence identity with AusE, but given the structural differences between 1 and austinol, PrhA should have a distinct activity from that of AusE. Thus, it seemed that PrhA accepts 6 but produces a different product, berkeleydione (2), probably via berkeleyone B²³ (7) (Scheme 1). The late-stage in the biosynthesis of 1 should involve the three P450s (PrhB, PrhD, and PrhN) and one isomerase (PrhC), but it is difficult to predict the pathway and the functions of each enzyme at this point. However, the first two steps after the formation of 2 could be proposed as follows: one of the P450s oxidizes the exomethylene of 2 into an aldehyde, which is then accepted by the putative isomerase PrhC to undergo retro-Claisen cleavage on the D-ring and recyclization to yield berkeleyacetal A (Figure S3).²

Reconstitution of Berkeleydione Biosynthesis in *Aspergillus oryzae*. To experimentally support the biosynthetic hypothesis for berkeleydione (2), we sought to analyze the functions of four oxidative enzymes, PrhI, PrhJ, PrhK, and PrhA. To this end, the four genes were introduced into a heterologous host, *Aspergillus oryzae* NSARI,²⁴ and the resulting transformants were cultivated in the presence of the substrate protoaustinoide A (3).⁵ The transformant with *prhI* alone transformed 3 into the new metabolite 4, which was not detected in the control strain (Figure 3A, lanes i and ii). Since the molecular weight of 4 was 2 Da smaller than that of 3, 4 was expected to be the 3-keto form of 3. The metabolite 4 was isolated and subjected to NMR analyses, which confirmed that 4, named protoaustinoide B, is indeed the analogue of 3 with a C-3 ketone functionality (Scheme 1, Table S3, and Figures S8 to S13). The two and three gene-expression systems with *prhI* and *prhJ*, without/with *prhK*, were subsequently analyzed, and the transformants produced preaustinoide A (5) and preaustinoide A1 (6), respectively (Figure 3B, lanes iii and iv, Tables S4 and S5, and Figures S14 to S25). Finally, the strain harboring all the four genes converted 3 into 2 (Figure 3A, lane vii), which was confirmed to be berkeleydione (Table S7, and Figures S32 and S37). We also detected and isolated berkeleyone B (7) from another four gene-containing transformant (Figure 3A, lane vi, Table S6, and Figures S26 and S31). These analyses demonstrated that PrhA has a different activity from that of AusE, and was suggested that PrhA produces 2 from 6, via 7, by constructing the cycloheptadiene system. The absolute configuration of 2 was established by the comparison of its

Scheme 1. Proposed Biosynthetic Pathway of Berkeleydione (2), Berkeleytrione (8), and Preaustinoid A3 (17)

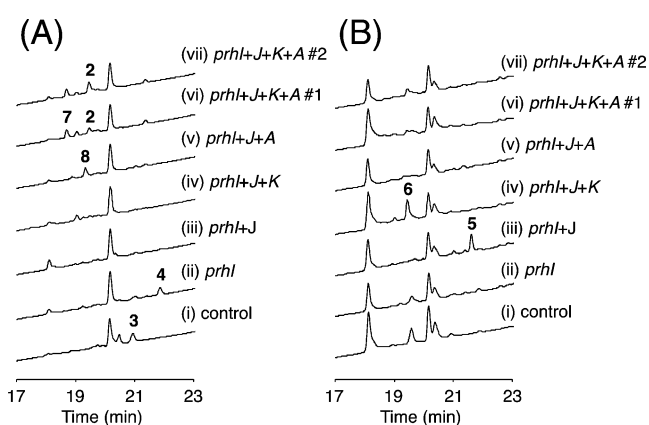
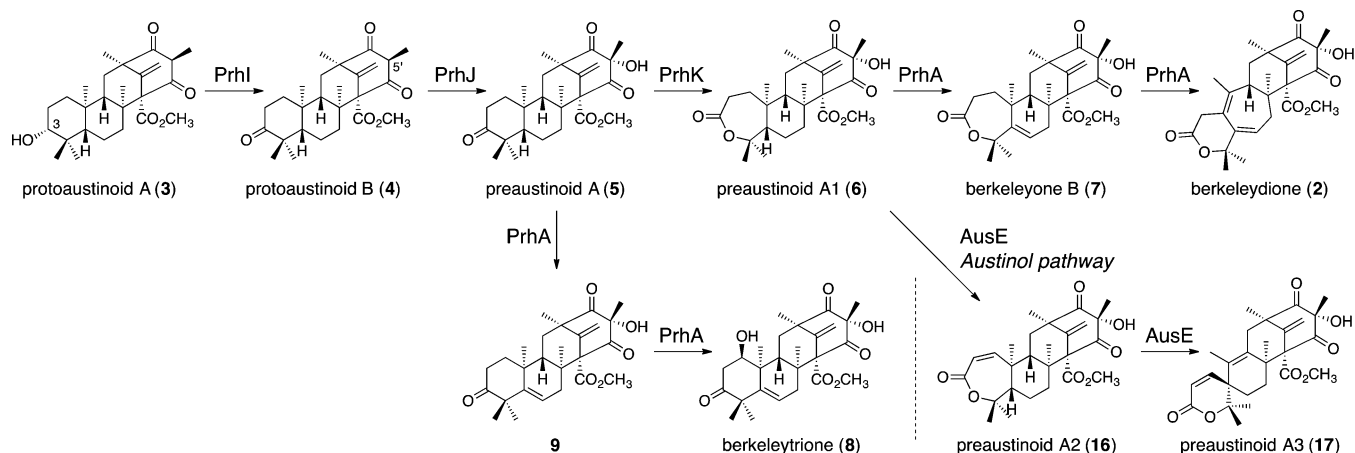


Figure 3. Biotransformation of protoaustinoid A (3). HPLC chromatograms of (A) culture supernatant extract and (B) mycelial extract from *A. oryzae* transformant incubated with 3: transformants harboring (i) empty vectors, (ii) *prhI*, (iii) *prhI + J*, (iv) *prhI + J + K*, (v) *prhI + J + A*, (vi) *prhI + J + K + A #1*, (vii) *prhI + J + K + A #2*. The chromatograms were monitored at 220 nm.

specific rotation with the reported one for berkeleydione,¹⁶ whose absolute configuration has been determined.¹⁷ This also allowed the confirmation of all the absolute configurations of the isolated compounds in this study as shown in Scheme 1.

We further constructed the three gene-expressing system lacking the FMO gene *prhK*, since the berkeleydione-producing fungus also yielded berkeleytrione (8),¹⁶ which seems to be synthesized without Baeyer–Villiger oxidation and to be generated by the oxidation of 5 by a PrhA-like dioxygenase. The transformant successfully produced the new metabolite 8 (Figure 3A, lane v), which was determined to be berkeleytrione (Scheme 1, Table S8, and Figures S38 and S43). Although we were unable to isolate the intermediate between 5 and 8, 8 should be produced via 9, which resembles 7 but lacks one oxygen atom (Scheme 1). Collectively, PrhA is a multifunctional dioxygenase that accepts both 5 and 6 to perform two sequential oxidations.

In Vitro Characterization of the Dioxygenase PrhA. To obtain deeper insight into the PrhA-catalyzed reaction, we performed an in vitro assay using the recombinant enzyme obtained from *Escherichia coli* expression system. PrhA is homologous to phytanoyl-CoA dioxygenase,²⁵ which requires Fe(II) and α -ketoglutarate (α -KG) for its activity, and therefore PrhA was incubated in the presence of FeSO_4 , α -KG, and

preaustinoid A1 (6). As expected, the production of berkeleydione (2) was observed only in the presence of PrhA (Figure 4A, lanes i and iv, and Figure S2). The enzymatic

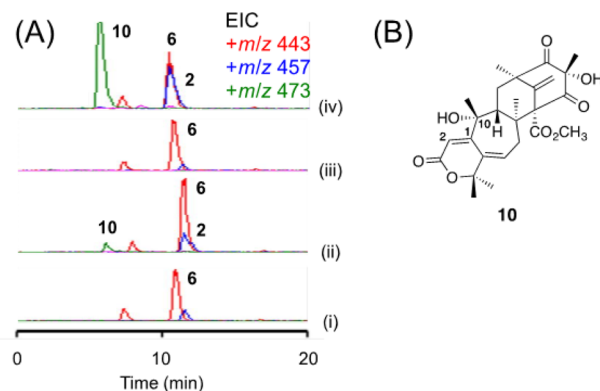
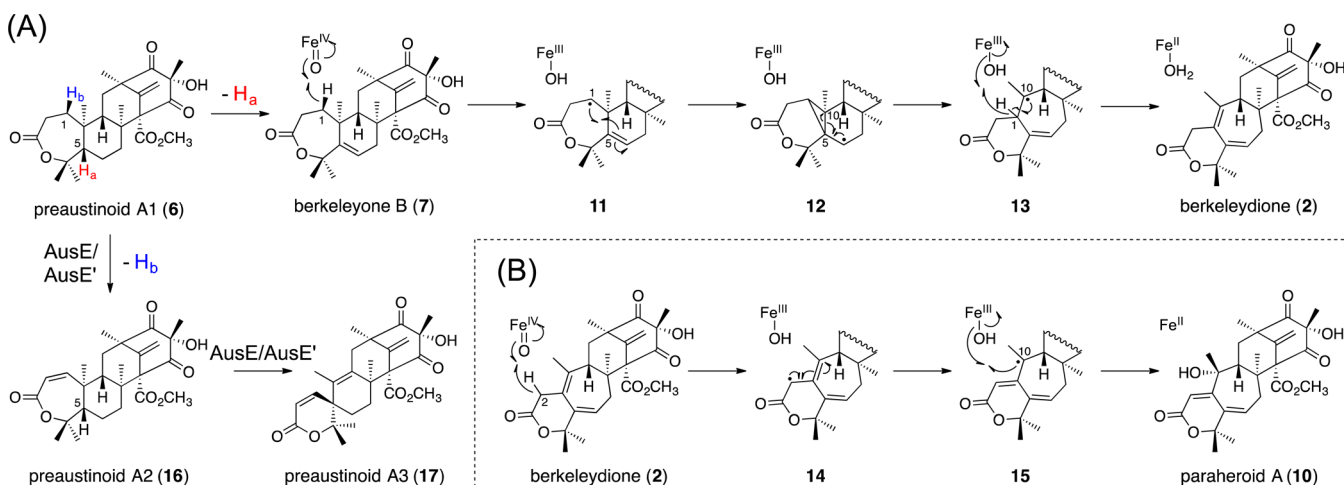


Figure 4. (A) LC–MS profiles of the products of in vitro enzymatic reactions of PrhA with 6: (i) without PrhA, (ii) without exogenous Fe(II), (iii) without α -KG, (iv) complete reaction. (B) Structure of compound 10.

reaction proceeded in the absence of exogenous iron with reduced activity, probably due to the remaining ferrous ion bound to the enzyme, but was abolished in the absence of α -KG (Figure 4A, lanes ii and iii), indicating that PrhA is an Fe(II)/ α -KG-dependent dioxygenase. Taken together, PrhA solely catalyzes the formation of the chemically intriguing cycloheptadiene by two successive oxidations.

Interestingly, the in vitro reaction yielded another product 10, which was not detected in the *A. oryzae* transformant. Since the molecular weight of 10 was 16 Da larger than that of 2, it was predicted that 10 is an oxygenated form of 2. Furthermore, unlike the other meroterpenoid species obtained in this study, 10 displayed maximal UV absorption at 276 nm (Figure S1), indicating a change in the conjugated system upon the generation of 10. The ¹H NMR spectrum of 10 revealed the occurrence of an olefinic proton at 6.00 ppm as well as the disappearance of two protons bound to C-2 of 2, suggesting that a double bond is newly installed between the C-1 and C-2 positions. Further analyses with ¹³C and 2D NMR spectra revealed the structure of 10, which possesses a dienone substructure and a α -hydroxyl group at the C-10 position (Figures 4B and S44 to S49 and Table S9). Interestingly, the A-

Scheme 2. Proposed Mechanism of PrhA-Catalyzed Reactions



and B-rings of compound **10**, designated as paraheroid A, are the same as those of dhilirolide D (Figure 1A).¹⁴

As seen in other Fe(II)/ α -KG-dependent dioxygenases, PrhA maintains a conserved 2-His-1-carboxylate iron-binding facial triad (H130, D132, H214) (Figure S7),²⁶ and therefore the iron atom at this site should play critical roles in the PrhA-catalyzed oxidations and structural rearrangement. The mechanism for the conversion from berkeleyone B (**7**) to berkeleydione (**2**) could be proposed as follows (Scheme 2A). Initially, α -KG and molecular oxygen are incorporated into the active site of the enzyme, and subsequent oxidative decarboxylation of α -KG leads to the generation of the highly active Fe(IV)-oxo species. The enzyme then abstracts the hydrogen atom from C-1 to yield the radical species **11**, which is further transformed into **13**, probably via the reaction known as homoallyl-homoallyl radical rearrangement.²⁷ In this process, the cyclopropylcarbinyl radical species **12** would serve as a reaction intermediate, and C-C bonds at C-1/C-5 and C-5/C-10 are respectively formed and cleaved to achieve the B-ring expansion. Finally, the abstraction of the hydrogen atom from C-1 of **13** finalizes the reaction to afford the cycloheptadiene skeleton of **2**.

AusE, the dioxygenase in the austinol pathway, also utilizes preaustinoid A1 (**6**) as a substrate to perform two rounds of oxidation.⁸ In the AusE-catalyzed reactions, the hydrogen atom at C-1 of **6** is initially abstracted to form the double bond between C-1 and C-2, and the C-5 hydrogen is then abstracted to initiate the spiro-ring formation. In contrast, PrhA abstracts the C-5 hydrogen and then the C-1 hydrogen in this order. Thus, although these two dioxygenases share the common substrate and both perform chemically interesting transformation probably by the homoallyl-homoallyl radical rearrangement,² the difference in the initial hydrogen abstraction appears to determine the rearrangement pattern and the end product of the reaction.

Additionally, the mechanism to afford paraheroid A (**10**) can also be proposed (Scheme 2B). In the predicted reaction, the C-2 hydrogen atom is initially abstracted to yield **14**, which undergoes double bond isomerization to give **15**. The oxygen rebound would complete the reaction to provide **10**. Although we were not able to detect **10** in the *A. oryzae* transformant, it is not clear whether the *P. brasilianum* strain produces **10**. Nevertheless, since paraherquinonin (**1**) possesses the same dienone substructure as **10**, PrhA is probably engaged in the

double bond isomerization in the paraherquinonin pathway. However, if **10** serves as the biosynthetic intermediate of **1**, then the C-10 hydroxyl group must be removed, probably by dehydration and olefin reduction, but the enzymes for these reactions are apparently not encoded by the *prh* cluster. Thus, some other enzymes encoded outside the *prh* cluster might also be involved in the paraherquinonin pathway.

Investigation of the Meroterpenoid Biosynthetic Gene Cluster in *P. brasilianum* MG11. After we obtained the genome sequence of *P. brasilianum* NBRC 6234, the genome sequence of another strain, *P. brasilianum* MG11, was published.²⁸ Interestingly, although these two strains belong to the same species, *P. brasilianum* MG11 reportedly produces austinol and its derivatives (Figure 1B),²⁹ and paraherquinonin (**1**) and the other meroterpenoids shown in Figure 1A have never been isolated from the fungus. We therefore sought to clarify the factor that differentiates the meroterpenoid productions in these two strains. Surprisingly, *P. brasilianum* MG11 possesses a gene cluster quite similar to the *prh* cluster, which was hereby designated as the *aus'* cluster (cluster A) for convenience (Figures 2 and S5). The eight predicted enzymes for the preaustinoid A1 synthesis, encoded by the *aus'* cluster, are almost identical to their corresponding Prh proteins (95–99% amino acid sequence identity). PrhA and the dioxygenase encoded by the *aus'* cluster, which was named AusE' (PMG11_09847; GenBank: CEJ61311.1), are less identical, but still share 92% protein sequence identity (Figure S5). Given that AusE' is the most homologous protein to AusE, among the proteins encoded by the *P. brasilianum* MG11 genome, and that the second most similar one shares only 36% protein sequence identity with AusE, it is most likely that AusE' is responsible for the spiro-lactone formation in *P. brasilianum* MG11.

To determine the function of AusE', the purified recombinant protein was prepared, and incubated with preaustinoid A1 (**6**) in the same manner as described for PrhA. As expected, AusE' accepted **6** as its substrate and produced the preaustinoid A3 (**17**) as AusE did, demonstrating that AusE' indeed possesses a distinct activity from that of PrhA (Figure 5 and Scheme 2). Unfortunately, due to the lack of the structural information for these dioxygenases, it remains uncertain which specific amino acid residues are actually critical for the reaction specificity; however, only slight mutation(s) of an enzyme can give rise to drastic changes in its product profile. The crystal structures of several Fe(II)/ α -KG-dependent

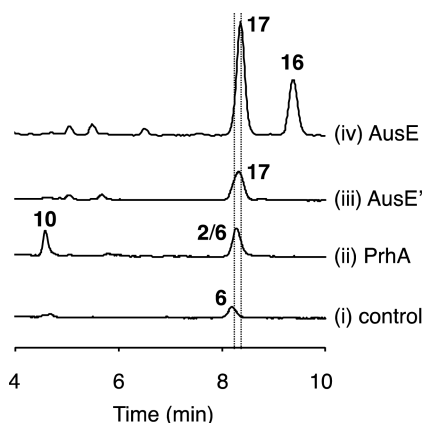


Figure 5. HPLC profiles of the products of in vitro enzymatic reactions, using **6** as a substrate: (i) without any enzymes, (ii) with PrhA, (iii) with AusE', (iv) with AusE. The chromatograms were monitored at 220 nm.

dioxygenases in fungal natural product pathways have recently provided important mechanistic insights into intriguing transformations, including the endoperoxide formation by FtmF/FtmOx1³⁰ and the quinolone generation by AsqJ.³¹ Thus, crystallization of PrhA and AusE (AusE') in the presence of different substrates, as well as mutational studies based on the structures, would definitely provide clues toward understanding the product selectivity of these dioxygenases and an opportunities to alter the functions of the enzymes.

Another interesting feature of the *aus'* cluster is that it lacks enzymes corresponding to PrhB, PrhC, PrhD, and PrhN apparently due to the omission of the DNA sequence in the corresponding region between *prhA* and *prhE*, as well as the mutation of the *prhN*-like gene (Figure 2). Alternatively, *P. brasilianum* MG11 has another gene cluster (cluster B) encoding enzymes nearly identical to those for the late-stage in the biosynthesis of austinol (Figures S5 and S6).³ Therefore, the *aus'* cluster B seems to be involved in the tailoring reactions in the late-stage of the biosynthesis of acetoxydehydroaustin, which is presumably the end product of the *aus'* pathway. Although the flanking regions of the second *aus'* cluster are also present in *P. brasilianum* NBRC 6234, the corresponding region of the *aus'* cluster B is replaced with a single gene (Figure S6). Thus, the production of austin family meroterpenoids in *P. brasilianum* MG11 could be attributed to the mutations in the *prh* cluster and the acquisition of another gene cluster for the late-stage in the biosynthesis.

CONCLUSION

In this study, we identified the biosynthetic gene cluster of paraherquonin (**1**), and revealed the pathway leading to berkeleydione (**2**). Fascinatingly, the dioxygenase PrhA catalyzes not only multistep oxidations but also the structural rearrangement to afford the cycloheptadiene moiety, providing a new repertoire for enzyme-catalyzed complex skeletal reconstructions. Furthermore, a protein highly homologous to PrhA was found in *P. brasilianum* MG11, which in turn is responsible for the spiro-lactone synthesis. These observations suggested that only slight mutations caused the pathway divergence in the same species. To further clarify the factors that define the catalytic differences, protein crystallization and mutational studies of PrhA and AusE are in progress in our laboratories. Finally, the late-stage of the biosynthesis of **1**

should also involve many intriguing chemical reactions. Therefore, the identification of the genes encoding the enzymes responsible for these transformations would provide more interesting enzymes and opportunities to artificially combine the *prh* and *aus* (*aus'*) genes to create new metabolic pathways, just as the *P. brasilianum* strains did in their evolutionary histories.

MATERIALS AND METHODS

Strains and Media. *Penicillium brasilianum* NBRC 6234 was obtained from the Biological Resource Center, National Institute of Technology and Evaluation (Chiba, Japan). *P. brasilianum* NBRC 6234 was cultivated at 30 °C, 160 rpm in DPY medium (2% dextrin, 1% hipolypepton (Nihon Pharmaceutical Co., Ltd.), 0.5% yeast extract (Difco), 0.5% KH₂PO₄, and 0.05% MgSO₄·7H₂O) for 3 days, and used as a source for whole genome sequencing and the cloning of each gene in the *prh* cluster.

Aspergillus oryzae NSAR1 (*niaD*⁻, *sC*⁻, Δ *argB*, *adeA*⁻)²⁴ was used as the host for fungal expression. Transformants of the *A. oryzae* strain were grown in shaking cultures in DPY medium for 3 days at 30 °C and at 160 rpm in the presence of protoaustinoid A (30 mg/L), which was prepared as previously described.⁵

Standard DNA engineering experiments were performed using *Escherichia coli* DH5 α , purchased from Clontech (Mountain View, CA). *E. coli* cells carrying each plasmid were grown in Luria–Bertani (LB) medium and selected with appropriate antibiotics. *E. coli* Rosetta2(DE3)pLysS (Novagen) was used for the expression of PrhA and AusE'.

Whole Genome Sequencing and Analysis. Genome sequencing of *P. brasilianum* NBRC 6234 was performed by Hokkaido System Science Co., Ltd. (Hokkaido, Japan) with an Illumina HiSeq 2000 system. Sequence assembly was performed with Velvet version 1.2.08³² (<http://www.ebi.ac.uk/~zerbino/velvet/>) to yield 1512 contigs covering approximately 33.8 Mb. Gene prediction was then performed with AUGUSTUS³³ (<http://bioinf.uni-greifswald.de/webaugustus/>) and manually revised by comparisons with homologous genes found in the NCBI database, if necessary. All of the products of the predicted genes were used to construct the database for the local BLAST search.

Construction of Fungal Expression Plasmids. For the construction of one-gene containing fungal expression plasmids, each gene in the *prh* cluster was initially amplified from *P. brasilianum* NBRC 6234 genomic DNA, with the primers listed in Tables S1 and S2. The full-length *prh* genes were purified, digested with appropriate restriction enzymes, and ligated into the pTAex3³⁴ or pUSA³⁵ vectors using a Ligation Kit Ver. 2.1 (TaKaRa) according to the manufacturer's protocol (Table S2). To construct the *prhI* and *prhA* coexpression plasmid, pTAex3-*prhA* was digested with *Bam*HI to yield the DNA fragment containing *PamyB*-*prhA*-*TamyB*. This fragment was ligated into pUSA-*prhI*, which had been digested with *Bam*HI and dephosphorylated, to produce pUSA-*prhI*+A. For the introduction of *prhJ* into pAdeA,³⁶ a fragment containing the *amyB* promoter (*PamyB*) and the *amyB* terminator (*TamyB*) was amplified from pTAex3-*prhJ*, digested with *Spe*I, and ligated into pAdeA (Table S2). To construct the *prhJ* and *prhK* coexpression plasmid, two different gene fragments with both *PamyB* and *TamyB* and with either *prhJ* or *prhK* were amplified from pTAex3-based plasmids and ligated into pAdeA, using an In-Fusion HD Cloning Kit (Clontech Laboratories, Inc.), to generate pAdeA-*prhJ*+K (Table S2).

Transformation of *Aspergillus oryzae* NSAR1. Transformation of *A. oryzae* NSAR1 was performed by the protoplast–polyethylene glycol method reported previously.³⁷ To coexpress *prhI*, *prhJ*, *prhK*, and *prhA*, two plasmids, pUSA-*prhI*+A and pAdeA-*prhJ*+K, were used for the transformation. For the construction of negative control strains that do not express one or more genes, the corresponding void vectors or plasmids with only one gene were used for the transformation.

HPLC Analysis of Each Product. Products from each of the transformants were analyzed by HPLC, with a solvent system of 0.5% acetic acid (solvent A) and acetonitrile containing 0.5% acetic acid

(solvent B), at a flow rate of 1.0 mL/min and a column temperature of 40 °C. Separation was performed with solvent B/solvent A (20:80) for 5 min, a linear gradient from 20:80 to 100:0 within the following 20 min, 100:0 for 5 additional min, and a linear gradient from 100:0 to 20:80 within the following 3 min.

Products from each of the in vitro reaction mixture were analyzed by HPLC, with a solvent system of 0.5% acetic acid (solvent A) and acetonitrile containing 0.5% acetic acid (solvent B), at a flow rate of 1.0 mL/min and a column temperature of 40 °C. Separation was performed with solvent B/solvent A (50:50) for 10 min.

LC–MS Analysis of Each Product. Products from each of the transformants and the in vitro reaction mixture were analyzed by LC–MS, with a solvent system of 1.0% acetic acid (solvent A) and acetonitrile containing 1.0% acetic acid (solvent B), at a flow rate of 0.2 mL/min and a column temperature of 20 °C. Separation was performed with solvent B/solvent A (50:50) for 5 min, a linear gradient from 50:50 to 75:25 within the following 15 min, and a linear gradient from 75:25 to 50:50 within the following 5 min.

Isolation and Purification of Each Metabolite. For the isolation of each metabolite, media from one liter of the culture were extracted with ethyl acetate. Mycelia were extracted with acetone at room temperature overnight, concentrated, and reextracted with ethyl acetate. Both extracts were combined and subjected to silica-gel column chromatography and further purification by preparative HPLC. The detailed purification procedures for each compound are described in [Supporting Information](#).

Expression and Purification of PrhA. To express *prhA* in *E. coli*, the gene was introduced into the pET-22b(+) vector (Novagen). The full-length *prhA* gene was amplified with the primers listed in [Tables S1 and S2](#), purified, digested with *NdeI* and *HindIII*, and ligated into the pET-22b(+) vector using T4 DNA ligase (TaKaRa) ([Table S2](#)).

For the expression of PrhA, *E. coli* Rosetta2(DE3)pLysS was transformed with the pET-22b(+)-*prhA* plasmid. The transformant was incubated with shaking at 37 °C/110 rpm, in LB medium supplemented with 100 mg/L of ampicillin sodium salt and 12.5 mg/L chloramphenicol. Gene expression was induced by the addition of 0.3 mM IPTG when the cultures had grown to an OD₆₀₀ of 0.6, after which the incubation was continued for 17 h at 16 °C/110 rpm. The cells were harvested by centrifugation, resuspended in lysis buffer (50 mM Tris, pH 7.5, 200 mM NaCl, 5 mM imidazole, 5% glycerol), and lysed on ice by sonication. The cell debris was removed by centrifugation, and the supernatant was loaded onto a 5 mL HisTrap HP column (GE Healthcare) pre-equilibrated with wash buffer (50 mM Tris, pH 7.5, 200 mM NaCl, 15 mM imidazole, 5% glycerol). After washing with 30 CV of wash buffer, the His-tagged protein was eluted with a linear gradient of 15 to 300 mM imidazole in the buffer. Further purification was achieved by gel-filtration chromatography, using a HiLoad 16/60 Superdex 200 prep grad (GE Healthcare) column with gel-filtration buffer (20 mM Tris, pH 7.5, 100 mM NaCl, 2 mM DTT). The purity of the enzymes was analyzed by sodium dodecyl sulfate polyacrylamide gel electrophoresis (SDS-PAGE). The protein concentration was determined using a NanoDrop ND1000 Spectrophotometer (Thermo Scientific).

Expression and Purification of AusE' and AusE. A synthetic gene encoding *ausE'*, which was codon-optimized for *E. coli* expression, was introduced into the pET-22b(+) vector. The full-length *ausE'* gene was amplified with the primers listed in [Tables S1 and S2](#), purified, digested with *NdeI* and *HindIII*, and ligated into the pET-22b(+) vector using In-Fusion HD Cloning Kit ([Table S2](#)). The expression and purification of *ausE'* were performed in the same manner as described for PrhA. The recombinant AusE protein was prepared as previously described.⁸

Enzymatic Reaction Assay of PrhA, AusE', and AusE. The enzymatic reaction of PrhA, AusE, or AusE with preaustinoide A1 (**6**) were performed in reaction mixtures containing 50 mM PIPES buffer (pH 7.5), 1 mM of **6**, 0.2 mM FeSO₄, 5 mM α -ketoglutarate, 4 mM ascorbate, and 11 μ M purified enzyme, in a final volume of 50 μ L. After an incubation at 30 °C for 6 h, the reaction was terminated by adding 50 μ L of methanol and mixed by vortex. After centrifugation, the supernatant was analyzed by HPLC or LC–MS/MS.

Analytical Data. Berkeleydione (2). White solid; $[\alpha]_{\text{D}}^{20} + 128.3$ (c 0.26, CHCl₃); for UV spectrum see [Figure S1](#); for ¹H and ¹³C NMR data see [Table S7](#) and [Figures S32 and S33](#); HR-ESI-MS found *m/z* 457.2225 [M + H]⁺ (calcd 457.2226 for C₂₆H₃₃O₇). The NMR data are in good agreement with the reported data.¹⁶

Protoaustinoide B (4). White solid; $[\alpha]_{\text{D}}^{20} -21.2$ (c 0.98, CHCl₃); for UV spectrum see [Figure S1](#); for ¹H and ¹³C NMR data see [Table S3](#) and [Figures S8 and S9](#); HR-ESI-MS found *m/z* 428.2566 [M]⁺ (calcd 428.2563 for C₂₆H₃₆O₅).

Preaustinoide A (5). White solid; $[\alpha]_{\text{D}}^{20} + 10.5$ (c 0.14, CHCl₃); for UV spectrum see [Figure S1](#); for ¹H and ¹³C NMR data see [Table S4](#) and [Figures S14 and S15](#); HR-ESI-MS found *m/z* 444.2521 [M]⁺ (calcd 444.2512 for C₂₆H₃₆O₆). The NMR data are in good agreement with the reported data.²¹

Preaustinoide A1 (6). Yellowish white solid; $[\alpha]_{\text{D}}^{20} -29.7$ (c 0.42, CHCl₃); for UV spectrum see [Figure S1](#); for ¹H and ¹³C NMR data see [Table S5](#) and [Figures S20 and S21](#); HR-ESI-MS found *m/z* 460.2440 [M]⁺ (calcd 460.2461 for C₂₆H₃₆O₇). The NMR data are in good agreement with the reported data.²²

Berkeleyone B (7). White solid; $[\alpha]_{\text{D}}^{20} -15.4$ (c 0.28, CHCl₃); for UV spectrum see [Figure S1](#); for ¹H and ¹³C NMR data see [Table S6](#) and [Figures S26 and S27](#); HR-ESI-MS found *m/z* 459.2381 [M + H]⁺ (calcd 459.2383 for C₂₆H₃₅O₇). The NMR data are in good agreement with the reported data.²³

Berkeleytrione (8). White solid; $[\alpha]_{\text{D}}^{20} -22.6$ (c 0.56, CHCl₃); for UV spectrum see [Figure S1](#); for ¹H and ¹³C NMR data see [Table S8](#) and [Figures S38 and S39](#); HR-ESI-MS found *m/z* 458.2284 [M]⁺ (calcd 458.2305 for C₂₆H₃₄O₇). The NMR data are in good agreement with the reported data.¹⁶

Paraheroid A (10). Amorphous solid; $[\alpha]_{\text{D}}^{22} -30.8$ (c 0.02, CHCl₃); for UV spectrum see [Figure S1](#); for ¹H and ¹³C NMR data see [Table S9](#) and [Figures S44 and S45](#); HR-ESI-MS found *m/z* 473.2185 [M + H]⁺ (calcd 473.2176 for C₂₆H₃₃O₈).

■ ASSOCIATED CONTENT

📄 Supporting Information

The Supporting Information is available free of charge on the ACS Publications website at DOI: 10.1021/jacs.6b08424.

Additional text with experimental details; 9 tables listing primers, plasmids, NMR data for **2**, **4–8**, and **10**; 49 figures showing UV spectra, mass spectra, a predicted biosynthetic pathway, information on the biosynthetic gene clusters, sequence alignment, and NMR spectra of **2**, **4–8**, and **10** (PDF)

■ AUTHOR INFORMATION

Corresponding Author

*abej@mol.f.u-tokyo.ac.jp

Author Contributions

‡Y.M. and T.I. contributed equally.

Notes

The authors declare no competing financial interest.

■ ACKNOWLEDGMENTS

We thank Prof. K. Gomi (Tohoku University) and Prof. K. Kitamoto (The University of Tokyo) for kindly providing the expression vectors and the fungal strain. This work was supported by Grants-in-Aid for Scientific Research from the Ministry of Education, Culture, Sports, Science and Technology, Japan (JSPS KAKENHI Grant Numbers JP16H06443, JP15H01836, and JP15K16554), by grant-in-aid from the Tokyo Biochemical Research Foundation, by Young Investigator Research Grant from Noda Institute for Scientific Research, and by the Sumitomo Foundation.

■ REFERENCES

- (1) Geris, R.; Simpson, T. J. *Nat. Prod. Rep.* **2009**, *26*, 1063–1094.
- (2) Matsuda, Y.; Abe, I. *Nat. Prod. Rep.* **2016**, *33*, 26–53.
- (3) Lo, H.-C.; Entwistle, R.; Guo, C.-J.; Ahuja, M.; Szewczyk, E.; Hung, J.-H.; Chiang, Y.-M.; Oakley, B.; Wang, C. C. *J. Am. Chem. Soc.* **2012**, *134*, 4709–4720.
- (4) Itoh, T.; Tokunaga, K.; Radhakrishnan, E. K.; Fujii, I.; Abe, I.; Ebizuka, Y.; Kushiro, T. *ChemBioChem* **2012**, *13*, 1132–1135.
- (5) Matsuda, Y.; Awakawa, T.; Itoh, T.; Wakimoto, T.; Kushiro, T.; Fujii, I.; Ebizuka, Y.; Abe, I. *ChemBioChem* **2012**, *13*, 1738–1741.
- (6) Guo, C.-J.; Knox, B. P.; Chiang, Y.-M.; Lo, H.-C.; Sanchez, J. F.; Lee, K.-H.; Oakley, B. R.; Bruno, K. S.; Wang, C. C. *Org. Lett.* **2012**, *14*, 5684–5687.
- (7) Matsuda, Y.; Awakawa, T.; Abe, I. *Tetrahedron* **2013**, *69*, 8199–8204.
- (8) Matsuda, Y.; Awakawa, T.; Wakimoto, T.; Abe, I. *J. Am. Chem. Soc.* **2013**, *135*, 10962–10965.
- (9) Matsuda, Y.; Wakimoto, T.; Mori, T.; Awakawa, T.; Abe, I. *J. Am. Chem. Soc.* **2014**, *136*, 15326–15336.
- (10) Matsuda, Y.; Iwabuchi, T.; Wakimoto, T.; Awakawa, T.; Abe, I. *J. Am. Chem. Soc.* **2015**, *137*, 3393–3401.
- (11) Okuyama, E.; Yamazaki, M.; Kobayashi, K.; Sakurai, T. *Tetrahedron Lett.* **1983**, *24*, 3113–3114.
- (12) Stierle, D. B.; Stierle, A. A.; Patacini, B. J. *Nat. Prod.* **2007**, *70*, 1820–1823.
- (13) Iida, M.; Ooi, T.; Kito, K.; Yoshida, S.; Kanoh, K.; Shizuri, Y.; Kusumi, T. *Org. Lett.* **2008**, *10*, 845–848.
- (14) de Silva, E. D.; Williams, D. E.; Jayanetti, D. R.; Centko, R. M.; Patrick, B. O.; Wijesundera, R. L.; Andersen, R. J. *Org. Lett.* **2011**, *13*, 1174–1177.
- (15) Centko, R. M.; Williams, D. E.; Patrick, B. O.; Akhtar, Y.; Garcia Chavez, M. A.; Wang, Y. A.; Isman, M. B.; de Silva, E. D.; Andersen, R. J. *J. Org. Chem.* **2014**, *79*, 3327–3335.
- (16) Stierle, D. B.; Stierle, A. A.; Hobbs, J. D.; Stokken, J.; Clardy, J. *Org. Lett.* **2004**, *6*, 1049–1052.
- (17) Stierle, A.; Stierle, D.; Decato, D. *Acta Crystallogr., Sect. E: Crystallogr. Commun.* **2015**, *E71*, o248–o248.
- (18) Etoh, T.; Kim, Y. P.; Tanaka, H.; Hayashi, M. *Eur. J. Pharmacol.* **2013**, *698*, 435–443.
- (19) Nielsen, M. L.; Nielsen, J. B.; Rank, C.; Klejnstrup, M. L.; Holm, D. K.; Brogaard, K. H.; Hansen, B. G.; Frisvad, J. C.; Larsen, T. O.; Mortensen, U. H. *FEMS Microbiol. Lett.* **2011**, *321*, 157–166.
- (20) Sullivan, M. J.; Petty, N. K.; Beatson, S. A. *Bioinformatics* **2011**, *27*, 1009–1010.
- (21) Geris dos Santos, R. M.; Rodrigues-Fo, E. *Phytochemistry* **2002**, *61*, 907–912.
- (22) Geris dos Santos, R. M.; Rodrigues-Fo, E. *Z. Z. Naturforsch., C: J. Biosci.* **2003**, *58*, 663–669.
- (23) Stierle, D.; Stierle, A.; Patacini, B.; McIntyre, K.; Girtsman, T.; Bolstad, E. *J. Nat. Prod.* **2011**, *74*, 2273–2277.
- (24) Jin, F. J.; Maruyama, J.; Juvvadi, P. R.; Arioka, M.; Kitamoto, K. *FEMS Microbiol. Lett.* **2004**, *239*, 79–85.
- (25) McDonough, M.; Kavanagh, K.; Butler, D.; Searls, T.; Oppermann, U.; Schofield, C. J. *Biol. Chem.* **2005**, *280*, 41101–41110.
- (26) Kovaleva, E. G.; Lipscomb, J. D. *Nat. Chem. Biol.* **2008**, *4*, 186–193.
- (27) Toyota, M.; Wada, T.; Fukumoto, K.; Ihara, M. *J. Am. Chem. Soc.* **1998**, *120*, 4916–4925.
- (28) Horn, F.; Linde, J.; Mattern, D. J.; Walther, G.; Guthke, R.; Brakhage, A. A.; Valiante, V. *Genome Announc.* **2015**, *3*, e00724–00715.
- (29) Hayashi, H.; Mukaiharu, M.; Murao, S.; Arai, M.; Lee, A. Y.; Clardy, J. *Biosci., Biotechnol., Biochem.* **1994**, *58*, 334–338.
- (30) Yan, W.; Song, H.; Song, F.; Wu, C.-H.; Her, A. S.; Pu, Y.; Wang, S.; Naowarajana, N.; Weitz, A.; Hendrich, M. P.; Costello, C. E.; Zhang, L.; Liu, P.; Zhang, Y. *Nature* **2015**, *527*, 539–543.
- (31) Bräuer, A.; Beck, P.; Hintermann, L.; Groll, M. *Angew. Chem., Int. Ed.* **2016**, *55*, 422–426.
- (32) Zerbino, D. R.; Birney, E. *Genome Res.* **2008**, *18*, 821–829.
- (33) Stanke, M.; Schöffmann, O.; Morgenstern, B.; Waack, S. *BMC Bioinf.* **2006**, *7*, 62.
- (34) Fujii, T.; Yamaoka, H.; Gomi, K.; Kitamoto, K.; Kumagai, C. *Biosci., Biotechnol., Biochem.* **1995**, *59*, 1869–1874.
- (35) Yamada, O.; Na Nan, S.; Akao, T.; Tominaga, M.; Watanabe, H.; Satoh, T.; Enei, H.; Akita, O. *J. Biosci. Bioeng.* **2003**, *95*, 82–88.
- (36) Jin, F.; Maruyama, J.; Juvvadi, P.; Arioka, M.; Kitamoto, K. *Biosci., Biotechnol., Biochem.* **2004**, *68*, 656–662.
- (37) Gomi, K.; Iimura, Y.; Hara, S. *Agric. Biol. Chem.* **1987**, *51*, 2549–2555.